PII: S1350-9462(98)00037-8

Progress in Measurement of Ocular Blood Flow and Relevance to Our Understanding of Glaucoma and Age-Related Macular Degeneration

A. Harris[a,*], H. S. Chung, T. A. Ciulla and L. Kagemann

Glaucoma Research and Diagnostic Center, Department of Ophthalmology, Indiana University, Indianapolis, IN 46202, USA and Department of Physiology and Biophysics, Indiana University, Indianapolis, IN 46202, USA

CONTENTS

Abstract 669
1. Introduction 670
2. Blood flow assessment 670
   2.1. Vessel caliber assessment 670
   2.2. Scanning laser ophthalmoscopic angiography 671
      2.2.1. Scanning-laser ophthalmoscopic fluorescein angiography 671
      2.2.2. Scanning-laser ophthalmoscopic indocyanine green angiography 671
   2.3. Laser doppler flowmetry 673
   2.4. Ocular pulse measurement 675
   2.5. Color doppler ultrasound imaging 676
3. Ocular hemodynamics in glaucoma 676
   3.1. Prevalence and pathogenesis of glaucoma 676
   3.2. Ocular perfusion defects in glaucoma 678
4. Ocular hemodynamics in age-related macular degeneration 680
   4.1. Prevalence and pathogenesis of age-related macular degeneration 680
   4.2. Ocular perfusion defects in AMD 681
5. Future trend 682
References 683

Abstract—New technologies have facilitated the study of the ocular circulation. These modalities and analysis techniques facilitate very precise and comprehensive study of retinal, choroidal, and retrobulbar circulations. These techniques include: 1. Vessel caliber assessment; 2. Scanning laser ophthalmoscopic fluorescein angiography and indocyanine green angiography to image and evaluate the retinal circulation and choroidal circulation respectively; 3. Laser Doppler flowmetry and confocal scanning laser Doppler flowmetry to measure blood flow in the optic nerve head and retinal capillary beds; 4. Ocular pulse measurement; and 5. color Doppler imaging to measure blood flow velocities in the central retinal artery, the ciliary arteries and the ophthalmic artery. These technique have greatly enhanced the ability to quantify ocular perfusion defects in many disorders, including glaucoma and age-related macular degeneration, two of the most prevalent causes of blindness in the industrialized world. Recently it has become clear, in animal models of glaucoma, that retinal ganglion cells die via apoptosis. The factors that initiate apoptosis in these cells remain obscure, but ischemia may play a central role. Patients with either primary open-angle glaucoma or normal-tension glaucoma experience various ocular blood flow deficits. With regard to age-related macular degeneration, the etiology remains unknown although some the-

*Corresponding author. Tel.: (317) 278-0134; Fax: (317) 278-1007; E-mail: Alharris@indiana.edu.

Progress in Retinal and Eye Research Vol. 18, No. 5, pp. 669 to 687, 1999

Printed in Great Britain
1350-9462/99/$ - see front matter

ories include primary retinal pigment epithelial senescence, genetic defects such as those found in the ABCR gene which is also defective in Stargardt's disease and ocular perfusion abnormalities. As the choriocapillaris supplies the metabolic needs of the retinal pigment epithelium and the outer retina, perfusion defect in the choriocapillaris could account for some of the physiologic and pathologic changes in AMD. Vascular defects have been identified in both nonexudative and exudative AMD patients using new technologies. This paper is a comprehensive update describing modalities available for the measurement of all new ocular bood flow in human and the clinical use.

1. INTRODUCTION

This paper attempts to provide the reader with a fundamental understanding of some of the methods used to evaluate ocular hemodynamics in glaucoma and age-related macular degeneration (AMD), two of the most prevalent causes of blindness in the industrialized world. The methods that will be discussed are vessel caliber assessment, scanning laser ophthalmoscopic angiography with fluorescein and indocyanine green dye, laser Doppler flowmetry, ocular pulse measurement and color Doppler imaging.

2. BLOOD FLOW ASSESSMENT

2.1. Vessel Caliber Assessment

Since the development of the ophthalmoscope, the retinal vessels have been evaluated for their health (Von Helmholz, 1951). The development of fundus photography gave researchers the means to more objectively assess retinal vessel diameters. The examination of fundus photographs under a microscope equipped with a micrometer reticle remained popular for many years. Hickam and his co-workers at Indiana University used this technique to demonstrate the vasoconstrictive effects of hyperoxia and later used this method as a measure of retinal vascular reactivity in health and disease (Hickam and Frayser, 1997; Hickam and Sieker, 1960; Sieker and Hickam, 1955; Sieker *et al.*, 1955). Others have used the same method to demonstrate reduced retinal vascular reactivity to oxygen in systemic hypertension (Ramalho and Dollery, 1968). Currently, fundus photographs are enlarged for measurement by projection (Bracher *et al.*, 1979; Delori *et al.*, 1988; Hodge *et al.*, 1969). Images of the fundus are projected from slides onto a screen at a known magnification and the vessel diameter is measured with calipers (Bracher *et al.*, 1979). A sophisticated micrometric technique has been developed using a rear-projection slide viewer. It projects the fundus image onto a translucent screen at a magnification of about 35× and is specially equipped with a thin wire which is positioned at the vessel edge by an operator while an interfaced computer calculates the diameter (Delori *et al.*, 1988).

A recent report placed intra-trial variability of project micrometry measurements between 1.6% and 2.9% depending on the experience of the observer (Delori *et al.*, 1988). Interobserver differences were much greater, as large as 11%. Considering the large interobserver differences with this technique, micrometry may be inadequate for accurately assessing vessel caliber. Because a variety of variables can alter the portion of the bloodstream devoted to the erythrocyte column versus that occupied by the marginal cell-free plasma zone (Bulpitt *et al.*, 1970), even the most reliable micrometric measure does not represent the entire blood column. These methods are also commonly used in conjunction with flow velocity measurements to calculate estimated volumetric blood flow in retinal vessels.

In order to measure vessel diameter in real units of length, individual eye magnification, the magnification of the camera or other imaging instruments must be known. The latter two vary by technique and instrument while the first varies from eye to eye. Commonly, particularly in studies with serial examinations, a single correction factor is applied to all eyes. While this does not affect detection of changes in diameter within a single eye, any diameter and resulting flow values should be expressed in unitless indices. In spite of this, physical units are often used with only a caveat in the method's description.

Recently, a new technique has been published which simplifies the method by computerizing the calculations based only on the eye's axial length

(Bennet *et al.*, 1994). It is important to keep in mind that the data obtained from vessel caliber measurements undergo a significant transformation before expressed in micrometers. Failure to account for magnification errors result in flawed absolute vessel measurements. The magnitude of the error is squared in the calculation of cross sectional vessel area. If an eye is its own control in a study, detection of trends in diameter will not be effected. Actual measurements will not be comparable between subject eyes due to natural variations in their optics, but changes in vessel size measured within a single eye will represent actual changes in vessel size.

2.2. Scanning Laser Ophthalmoscopic Angiography

The recent introduction of the scanning laser ophthalmoscope (SLO) (Nagel *et al.*, 1992; Webb *et al.*, 1987; Webb *et al.*, 1980), has brought quantitative angiography to new heights (Gabel *et al.*, 1988; Nakahashi, 1990; Nasemann and Müller, 1990). This instrument overcomes many of the limitations of traditional photographic or video angiography. The incandescent light source has been replaced with a low power scanning argon laser beam which allows better penetration through lens and corneal opacities. The beam passes through the center of the pupil and is focused at the retina to a point size of about 8 to 15 μm (Plesch *et al.*, 1990; Rehkopf *et al.*, 1990). This limit is set by the optical properties of the human eye. Overall retinal illumination is reduced and contrast is improved as only a single spot is illuminated by the laser beam at any moment.

The SLO is a confocal laser device. Reflected light exits the eye through the pupil and must pass through a confocal aperture before reaching a solid-state detector. This detector generates a voltage level based on the intensity of incoming light. The detector voltage level, measured in real time, creates the standard video signal. Scattered light and light reflected from sources outside of the focal plane is blocked by the confocal aperture. In angiography mode, the aperture is fully open. The signal is generally passed through a video timer and then directed to an S-VHS video recorder. The resulting images are similar to those obtained with standard video angiography, but with improved spatial resolution and contrast.

The SLO is available for fluorescein angiography as well as indocyanine green angiography. The examiner can select an integrated argon-blue laser (488 nm) with barrier filter (530 nm) for fluorescein angiography and an infrared diode laser (790 nm) with a barrier filter (830 mm) for indocyanine green angiography.

2.2.1. *Scanning-Laser ophthalmoscopic fluorescein angiography*

Fluorescein angiogram (Fig. 1) can be analyzed to obtain hemodynamic measurements such as arteriovenous passage (AVP) time and mean dye velocity (MDV). AVP time, analogous to mean circulation time, can be computed by comparing the times of dye arrival at the measuring point on the artery with that on the vein. MDV can be calculated by placing a second measuring window a known distance downstream on the artery from the first arterial measuring window (with no intervening branches). Because the distances involved are small, the time required for the dye's travel is short. This measure, MDV, could be performed only with high temporal resolution (0.03 s). The dramatic increase in temporal resolution with scanning laser ophthalmoscope permits another hemodynamic measure which is the visualization of hyper- and hypo-fluorescent segments in the perifoveal and superficial optic nerve head capillary circulation. These dark and light segments can easily be seen as they course the capillaries during visual inspection of the angiograms. It is possible to compute their velocity by measuring the distance they travel on successive frames and counting the number of frames needed for their travel using an image analysis system.

2.2.2. *Scanning-Laser ophthalmoscopic indocyanine green angiography*

Although choroidal blood flow has been described with fluorescein angiography, this technique has several limitations (Maumenee, 1968; Archer *et al.*, 1970; Duijm *et al.*, 1997). Because

Fig. 1. Twenty degree fluorescein retinal angiogram using scanning laser ophthalmoscopy.

the choroid supplies the majority of ocular blood flow, especially for the outer retinal layers and optic nerve, a better evaluation method for this important vasculature was needed. Indocyanine green (ICG) angiography, introduced by Flower and Hochheimer, and SLO technique have overcome some problems of fluorescein angiography in the study of choroidal blood flow (Flower and Hochheimer, 1972; Flower, 1972). The near-infrared light used for scanning-laser ICG angiography is much more efficient in its penetration of pigmented layers of the fundus as compared with the shorter wavelength used in fluorescein angiography (Wald, 1949; Geeraets *et al.*, 1960; Behrendt and Wilson, 1965). A second advantage is ICG dye's tendency to bind to plasma proteins. Approximately 98% of the dye is bound to plasma albumin or lipoprotein (Cherrick *et al.*, 1960; Baker, 1966). As a result, ICG diffuses slowly out of the fenestrated choriocapillaris in contrast to the rapid leakage of fluorescein dye, which prevents choroidal details. High-resolution ICG images can now be produced by scanning laser ophthalmoscopy.

While SLO clearly represents a major improvement in choroidal angiography, to obtain quantitative measurements, an additional digital image analysis system is needed. Unfortunately, while the SLO and several image analysis systems are commercially available, image analysis software does not come "off the shelf" ready to produce AVP times and MDV. This inhibits the widespread clinical application of scanning laser ophthalmoscopic angiography for quantitative choroidal hemodynamic assessment. The glaucoma research and diagnostic center in Indiana University has developed a new analysis technique to quantify choroidal ICG angiography using scanning laser ophthalmoscope. The entire 40° ICG angiogram is divided into a number of small regions, and dilution curves are created for each region. While it is difficult to use fluorescence to measure the exact concentration of ICG within the choroid, simultaneous acquisition of dye dilution curves from different locations within the choroid from a single angiographic exam allows comparison of relative concentrations between different locations. Six locations,

each a 6° square, on the image are identified for analysis (Fig. 2). The average brightness of the area contained in each box is computed for each frame of the angiogram (Fig. 3). Area brightness is graphed with time on the X axis and brightness on the Y axis. Area dye-dilution analysis identifies three parameters from the brightness maps: 10% filling time, the slope of curve, and maximum intensity of brightness (Fig. 3). First, the 10% filling time is the amount of time required to reach a brightness 10% above baseline. This parameter indicates rapidity of the early choroidal filling phase. Second, the slope is calculated with an intensity difference between 10% and 90% divided by the number of frames during that time. This parameter represents the overall speed of blood as it enters the choroid. Finally maximum intensity of brightness which indicates the vascular density of the area. For each parameters, the six curves are analyzed individually, as a mean of the six areas, and as the regional spread, or maximum value minus minimum value. Peripapillary and macular values are also compared for each parameter.

2.3. Laser Doppler Flowmetry

Laser Doppler Flowmetry (LDF) measures the amount and the velocity of moving red blood cells by using the optical Doppler effect (Riva *et al.*, 1989a). The Doppler effect is a frequency shift of a wave reflected from a moving object. The frequency shift is proportional to the velocity of the moving object. The object's velocity can be measured by measuring the amount of Doppler shift. Laser Doppler Flowmetry is a non-invasive technique that permits the assessment of relative blood velocity, volume and flow within a sampled volume of tissue. By directing the laser beam onto the retina or optic nerve head away from visible vessels, the Doppler shift in the returning

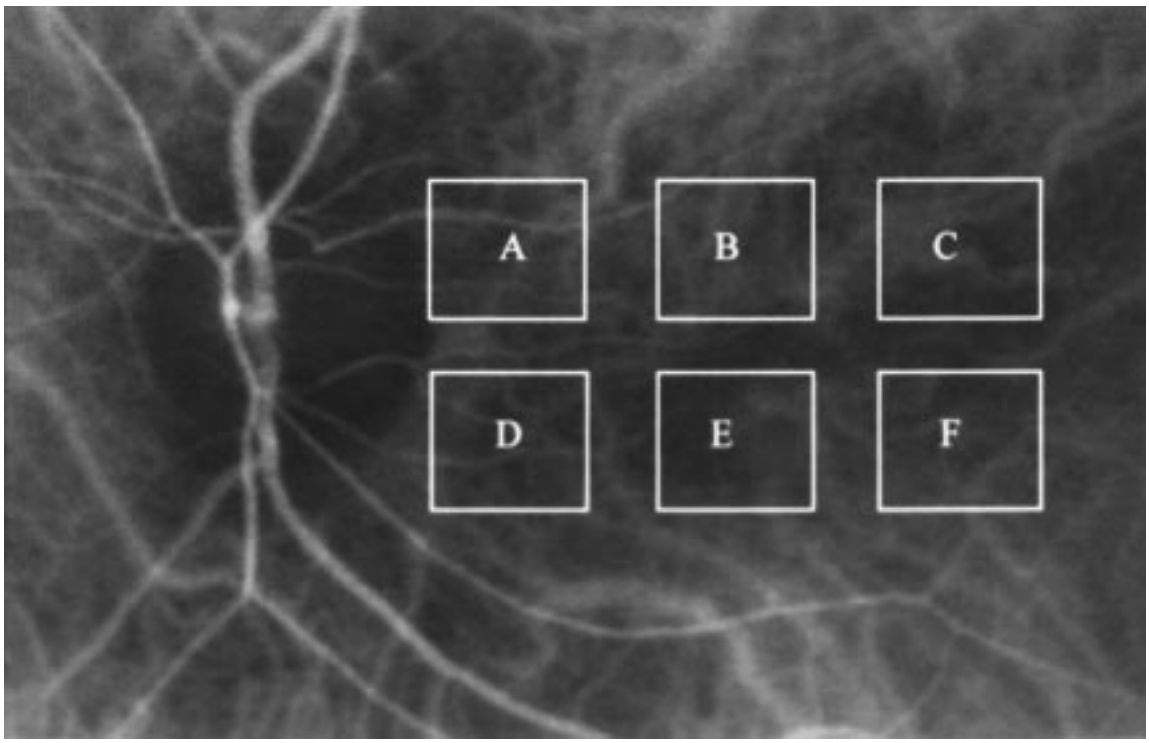

Fig. 2. Forty degree indocyanine green choroidal angiogram using scanning laser ophthalmoscopy. Six locations, each a 6° square, on the image are identified for area dilution analysis. A and D for peripapillary choroid, and B, C, E and F for macular area.

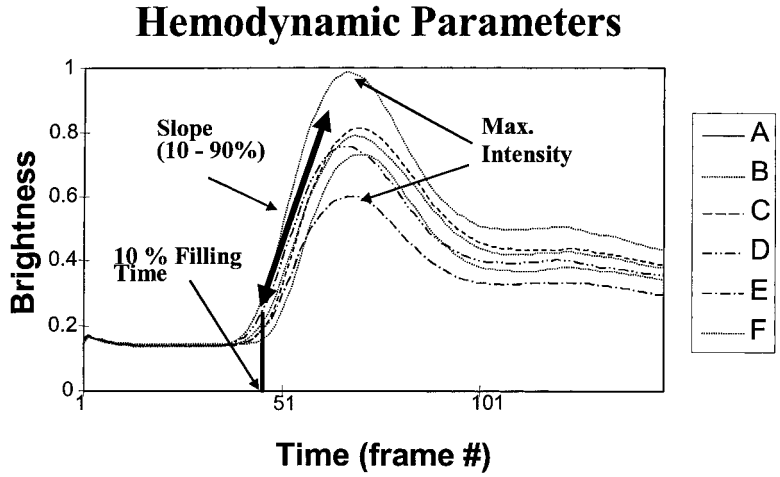

Fig. 3. Hemodynamic parameters in area dilution analysis of indocyanine green choroidal angiography using scanning laser ophthalmoscopy. Area dye-dilution analysis identifies three parameters from the brightness maps: 10% filling time, the slope of each curve, and the maximum intensity of brightness. The 10% filling time is the amount of time required to reach a brightness 10% above baseline. The slope is calculated with intensity difference between 10% and 90% divided by the number of frames during that time.

light scattered by moving blood cells could be analyzed to determine the blood velocity in the microvessels. Since the blood flow through the capillaries illuminated by the laser is in random directions, only an approximation of blood flow velocity can be made.

While the frequencies in the Doppler-shifted spectra are in proportion to the velocity of the blood cells, the intensity of the signal at each frequency in the spectra is proportionate to the number of cells traveling at that velocity. With knowledge of not only the flow velocity of blood but also the amount of blood traveling at that flow velocity, volumetric blood flow can be calculated. A number of commercially-available laser Doppler flowmeters operate in this fashion. The result is a display of blood velocity, volume and flow through the tissue sampled by the laser beam. Originally, use of the retinal laser Doppler flowmeter was limited to animal studies because of the intensity of the laser light. Experiments with the method in minipigs and cats have shown changes in optic nerve head blood flow in response to varied blood carbon dioxide levels (Riva *et al.*, 1989b), carotid occlusion (Riva *et al.*, 1989b), hyperoxia, and flicker stimulation (Riva *et al.*, 1992). Rhythmic changes in optic nerve head blood flow similar to those found in human skin have also been demonstrated with retinal laser Doppler flowmetry (Riva *et al.*, 1990).

Laser Doppler flowmeter (Oculix, Switzerland) has been adapted for human use (Cranstoun *et al.*, 1994; Harris *et al.*, 1996a; Joos *et al.*, 1994; Petrig and Riva, 1988). Measures of optic nerve head blood flow in the two eyes of the same subjects has been found to be significantly correlated and to decrease with increasing age (Cranstoun *et al.*, 1994). Hyperoxia and hypercapnea have also been shown to change optic nerve head blood flow as well as choroidal blood flow in the foveal region as measured with the technique (Harris *et al.*, 1996a).

Recently confocal scanning laser Doppler flowmetry (CSLDF) (HRF, Heidelberg Retinal Flowmeter, Heidelberg, Germany) has been developed and is actively used in ocular hemodynamic studies (Michelson *et al.*, 1996; Michelson and Schmauß, 1995; Chungs *et al.*, 1999). CSLDF is the combination of a laser Doppler flowmeter with a confocal scanning laser tomograph. CSLDF images a 2560×640 μm^2 area (256 points $\times$ 64 lines), 400 μm depth, of retina or optic nerve head with a measurement accuracy of 10 μm. Every line is scanned with a 790 nm laser,

128 times at a line sampling rate of 4000 Hz. After the scan is completed, the HRF computer performs a fast Fourier transform to extract the individual frequency components of the reflected light. For each point of the scan, a frequency spectrum is calculated. Each frequency location on the χ axis of the spectrum represents a blood velocity, and the height of the spectrum at that point represents the number of blood cells required to produce that intensity. Integrating the spectrum yields total blood flow. The instrument has been configured to analyze 10×10 pixel (100×100 μm) sized box of tissue. The CSLDF accurately measured blood flow in an artificial capillary tube ($r = 0.97$, $P < 0.0001$), providing results similar to commercially-available LDFs. The method also displayed coefficients of reliability near 0.85 for acutely repeated volume, velocity and flow measurements from 10×10 pixel sampling sites (Michelson and Schmauß, 1995). However, long-term reproducibility from these small sampling boxes is inadequate, with the coefficient of variation of measures repeated each week for four weeks averaging 30% of the mean (Kagemann *et al.*, 1998). Furthermore, using values collected with the conventional 10×10 pixel size, supplied by the manufacturer, perfusion of such small areas may not represent blood flow of whole retina. Therefore, the glaucoma research and diagnostic center in Indiana University has developed a pixel-by pixel analysis method which examines qualifying individual pixels from the entire 256×64 pixel image (Fig. 4). Large vessels, peripapillary atrophic regions, and image areas interrupted by movement saccades are avoided. To produce a histogram, the total number of pixels for all images is determined and an average calculated. Each image pixel count is then matched to the overall average and a normalized pixel count is calculated, giving equal weight to each subject. Flow, volume and velocity data at the 25th, 50th, 75th and 90th percentiles are used for analysis. Percentage of zero flow pixels is also calculated. Broadening the analysis to include every qualifying pixel within the entire image improves test/retest reliability, reducing the coefficient of variation of repeated weekly measurements to 15% for selected portions of the flow histogram.

2.4. Ocular Pulse Measurement

The relationship between the observable pulsatile change in IOP during the cardiac cycle and the resulting changes in ocular volume have been studied since 1962 (Eisenlohr and Langham, 1962; Eisenlohr *et al.*, 1962; Langham and Eisenlohr, 1963; Langham *et al.*, 1989a; Langham and Tomey, 1978; Silver *et al.*, 1989). Based on the volume pressure relationship, Langham developed the Ocular Blood Flow (OBF) device which calculates the real time change in ocular volume based on the real time measurement of IOP (Langham, 1987; Langham *et al.*, 1989b). If pulsation in IOP is due to blood surging into the eye during systole, then some unknown percentage of total ocular blood flow may be measurable. It is thought that the pulsatile component of ocular blood flow is that portion delivered during systole. Diastolic flow is the steady flow delivered during diastole accounting for perhaps two-thirds of total ocular flow (Langham *et al.*, 1989b).

The Langham OBF consists of a modified pneumo-tonometer interfaced with a microcomputer which records the ocular pulse (Langham *et al.*, 1991). The pulse wave is the rhythmic change in IOP during the cardiac cycle which exhibits a nearly sinusoidal pattern with a range of up to 2 mmHg. The OBF exam procedure consists of the placement of the tonometer on the cornea for several seconds. The pneumotonometer sends an analog signal to the computer where it is digitized and recorded. The amplitude of the IOP pulse wave is used to calculate the change in ocular volume. Calculations are based on the relationship described by Silver *et al.*, 1989. Recently the OBF system (OBF Labs Ltd, UK) which is similar to Langham ocular blood flow system has been introduced. The OBF Labs POBF system has rapidly gained popularity for use in ocular blood flow studies because it is fast, easy to use, relatively inexpensive and operates with acceptable reproducibility (Butt and O'Brien, 1995; Yang *et al.*, 1998).

There are several limitations which plague both systems. POBF values are not obtained through direct measurement of ocular blood flow, but derived mathematically by estimating ocular pulse volume change based on preset equations relating

ocular volume to IOP. This formula is based on the cardiac cycle and a standard scleral rigidity. POBF measurements are therefore affected by individual differences of scleral rigidity, ocular volume, heart rate, systemic blood pressure and IOP. For example, myopic eyes which have less scleral rigidity and larger ocular volume may have lower POBF measurement compared to normal or hyperopic eyes. Understanding these limitations is essential to proper study design and data interpretation. POBF may be more useful for studying intra-individual blood flow changes (i.e., before and after medication comparison) rather than inter-individual comparison (i.e., glaucoma patients versus normal subjects).

2.5. Color Doppler Ultrasound Imaging

A-scan ultrasound is commonly used to measure the eye's axial length. B-scan ultrasound has been used to produce gray-scale images of ocular structures for a number of years. Color Doppler imaging (CDI) is an ultrasound technique that combines B-scan gray scale imaging of tissue structure, color representation of blood flow based on Doppler shifted frequencies and pulsed-Doppler measurement of blood flow velocities (Powis, 1988; Taylor and Holland, 1990). Originally developed for imaging of blood flow in the heart and larger peripheral vessels, the applicability of CDI for measurement of blood flow velocities in orbital vessels has been documented by a number of researchers (Gutoff *et al.*, 1991; Lieb *et al.*, 1991; Williamson, 1994; Williamson and Harris, 1996).

Color Doppler imaging systems are unique in that they use a single multi-function probe to perform all functions. Sound waves are sent from the probe at a given frequency, generally 5 to 7.5 MHz. As in the other Doppler-based methods, blood flow velocity is determined by the shift in the frequency of the returning sound waves. Color is added to the familiar B-scan gray-scale image of the eye's structure to represent the motion of blood through vessels. The color varies in proportion to the flow velocity. Most units code red-to-white for motion toward the probe and blue-to-white for motion away from the probe.

The color Doppler image (Fig. 5) allows the operator to identify the desired vessel and place the sampling window for pulsed-Doppler measurements. These measurements display Doppler-shifted sound frequencies coming from the location of the sampling window. Flow velocity data is graphed against time. The peak and trough of the wave are identified by the operator. From these, the computer calculates peak systolic (PSV) and end diastolic (EDV) velocities. Additionally, Pourcelot's resistive index can be calculated as a measure of downstream vascular resistance according to the formula (Pourcelot, 1975):

$$RI = \frac{PSV - EDV}{PSV}$$

This index varies from zero to one, with higher values indicating higher distal vascular resistance.

In vitro studies have established the validity of Doppler ultrasound measures of flow velocity (Von Bibra *et al.*, 1990). Reproducibility has also been studied (Chang *et al.*, 1994; Flaharty *et al.*, 1994; Taylor and Holland, 1990), with best measures in the ophthalmic artery (coefficients of variation ranging from 4% for resistive index to 11% for peak systolic velocity). A potential source of error in ophthalmic CDI is excessive pressure applied to the eyelid. This pressure can result in a significant change in IOP and can lead to changes in perfusion pressure and blood flow (Harris *et al.*, 1996b).

3. OCULAR HEMODYNAMICS IN GLAUCOMA

3.1. Prevalence and Pathogenesis of Glaucoma

By the year 2000, an estimated 2.47 million Americans will suffer from primary open-angle glaucoma (Quigley and Vitale, 1997). Among persons over age 65, glaucoma represents the third most frequently reported reason for visits to physicians for a disease among all causes, and is the most frequent diagnostic code for ophthalmic vis-

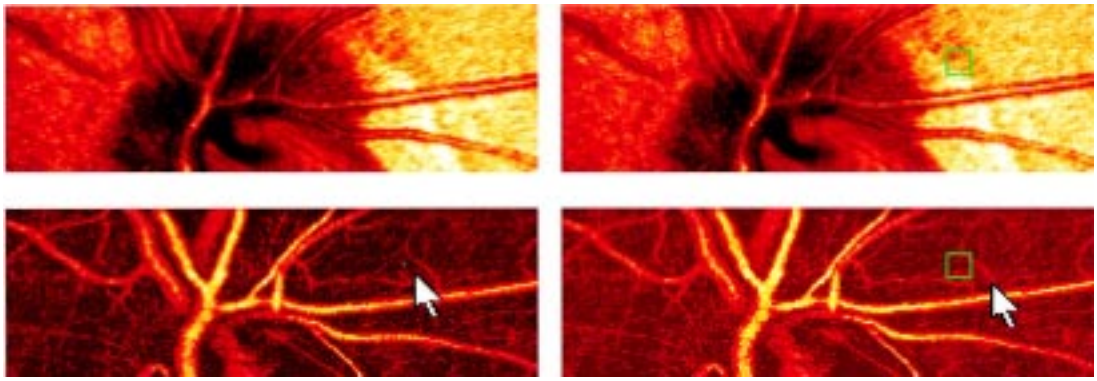

Fig. 4. Confocal scanning laser Doppler flowmetry (Heidelberg Retinal Flowmeter) of optic nerve head and peripapillary retina. The left arrow indicates an 1×1 pixel measurement window, which collects follow values from the entire retina except for large vessels, for new pixel-by pixel analysis. The right arrow indicates a 10×10 pixel measurement window used for conventional analysis.

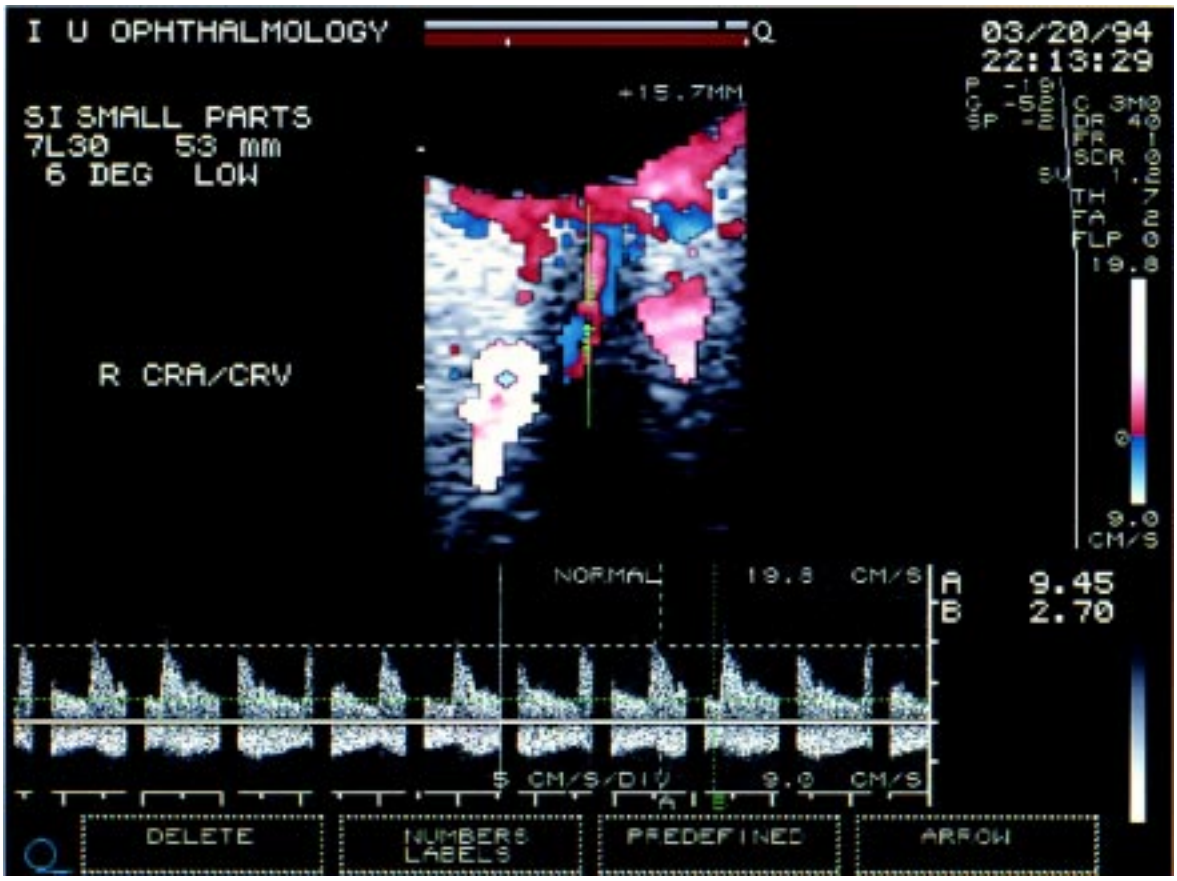

Fig. 5. Color Doppler image of the central retinal artery and vein taken with a 7.5 MHz linear probe (Siemens Quantum 2000 system). The Doppler shifted spectrum (time velocity curve) is displayed at the bottom of the image. Red and blue pixels represent blood movement toward and away from the transducer, respectively.

its among persons in the Medicare age group (Quigley and Vitale, 1997; Schappert, 1995).

Despite its prevalence, glaucoma remains a disease of unknown etiology and inadequate treatment (Tielsch, 1996). Although elevated intraocular pressure (lOP) was identified as the primary risk factor for the illness over 100 years ago, a meta-analysis of studies of pressure reduction carried out over the past seven decades shows that of 971 patients treated, 550 (57%) showed steady disease progression, with persons at all levels of lOP equally likely to exhibit deterioration (Chauhan, 1995). Indeed, these authors conclude that "factors quite independent of intraocular pressure may be responsible for [disease] progression in glaucoma" (Chauhan, 1995.

Patients with either primary open-angle glaucoma (POAG) or normal-tension glaucoma (NTG) evidence various ocular blood flow deficits. Recently it has become clear, in animal models of glaucoma, that retinal ganglion cells die via apoptosis (Quigley *et al.*, 1995). The factors that initiate apoptosis in these cells remain obscure. There are two major theoretical pathways for apoptotic retinal ganglion cell death: glutamate-mediated toxicity and neurotrophin withdrawal (Nickell, 1996). 1) Glutamate-mediated toxicity is a primary response to cellular ischemia. Thus, the hypothesis that glutamate toxicity plays an important role in stimulating ganglion cell death is consistent with an ischemic mechanism of optic nerve damage. 2) Neurotrophin withdrawal can be explained either by mechanical pressure due to increased IOP or by defective neurotrophin transport by energy depletion due to ischemia. In both of these pathways, ischemia plays a central role. It is logical to assume that alleviating ischemia will prove beneficial for glaucoma treatment.

3.2. Ocular Perfusion Defects in Glaucoma

Despite the central role that ischemia plays in apoptotic retinal ganglion cell death and the growing evidence that glaucoma patients suffer from inadequate ocular blood flow, current diagnostic procedures and clinical management of glaucoma do not take these considerations into account. Therefore, recent editorials have called for the evaluation of ocular circulation in glaucoma and a plethora of research has emerged examining the relationship between ocular hemodynamics and progression of the disease. This literature has emerged within the past two decades from technological developments that have led to a variety of non-invasive and minimally-invasive methods to assess ocular hemodynamics in humans. Understanding the origins of the data and appreciating their limitations can be difficult. Modern hemodynamic assessment techniques each examine a unique facet of the ocular circulation. No single facet provides a complete description of the hemodynamic state of the eye.

Vessel caliber assessment has been employed to evaluate vascular abnormalities in glaucoma. As noted above, fundus photographs are enlarged for measurement by projection. Images of the fundus are projected from slides onto a screen at a known magnification and the vessel diameter is measured a sophisticated micrometric. Jonas *et al.* reported that in the glaucoma group (473 eyes of 281 patients), the parapapillary retinal vessel caliber was significantly smaller than in the normal eyes (275 eyes of 173 subjects) (Jonas *et al.*, 1989). The differences were more marked for the arteries and the inferior temporal vessels compared to the veins and the superior temporal vessels, respectively. The vessel diameters decreased significantly with increasing glaucoma stage independently of the patients' age. In a study by Grunwald, the effect of topical timolol maleate 0.5% on the retinal circulation was investigated in normal subjects using the same method. No significant change in venous diameter was detected (Grunwald, 1991).

Scanning laser ophthalmoscopic fluorescein angiography has provided important information on retinal hemodynamics in normal and glaucoma subjects. In healthy subjects, arteriovenous passage times measured by scanning laser ophthalmoscopic angiography has been reported as averaging 1.58 ± 0.4 seconds and mean dye velocity averaging 6.67 ± 1.59 mm/sec in a large study of 221 individuals (Wolf *et al.*, 1994). In the same study, capillary flow velocity averaged 2.89 ± 0.41 mm/sec in 90 healthy subjects. On

repeated tests in the same group of 52 healthy subjects, arteriovenous passage time varied by an average of 15.6% and mean dye velocity by 16.7% (Wolf *et al.*, 1994). Capillary flow velocity varied 7.9% between two tests in the same 17 normal subjects. Wolf *et al.* used an SLO to evaluate retinal blood velocities of medically treated POAG patients and matched controls. They found an 11% reduction in the mean dye velocity within major retinal arteries. They also noted that arteriovenous passage time within retina was 41% slower in POAG (Wolf *et al.*, 1993). Topical carbonic anhydrase inhibitor, Dorzolamide has been shown to increase retinal arteriovenous passage time in glaucoma patients in an SLO study, however, using CDI no significant effect was observed on the retrobulbar vessels (Harris *et al.*, 1999).

Scanning-laser ophthalmoscopic ICG angiography has also been used to investigate ocular hemodynamics. Several authors have attempted to quantify morphologic and dynamic parameters in the choroidal circulation. In a recent study using a new area dilution analysis technique, ICG angiograms were recorded from 11 NTG patients and 12 age and IOP matched normal subjects (Chung *et al.*, 1998). There was no significant difference between normals and NTG patients in mean of slope, 10% filling time, or maximum intensity of brightness. The range of values across the six areas, which is the difference between maximum and minimum values, was significantly greater in NTG patients than in normals (2.86 vs. 1.39 s, $P = 0.01$). Difference of 10% filling time between peripapillary and macular area (mean of A and D vs mean of B, C, E and F in Fig. 2, respectively) was significantly greater in NTG patients than in normals (2.80 vs. 1.25 s, $P = 0.007$). The results from the study showed that early choroidal filling pattern is homogenous in normal subjects, but heterogeneous in NTG patients. In addition, peripapillary choroidal filling was delayed in NTG patients but not in normal subjects. These findings suggest that NTG patients may suffer from hypoperfusion of the choroid.

As noted earlier, confocal scanning laser Doppler flowmetry (CSLDF) has recently been developed and has shown hemodynamic alterations in glaucoma. In a recent study comparing age matched controls with NTG patients, a new pixel-by pixel analysis, which have been described earlier, showed that normal tension glaucoma patients presented with significantly lower blood flow than did age-matched normals (Chung *et al.*, 1999). In histograms utilizing every pixel from the peripapillary retina, NTG patients displayed significantly lower flow in the 25th, 50th and 75th percentile flow pixel (each $P < 0.05$) than did age-matched controls. These results were not detectable using conventional (default 10×10 pixel sized box) CSLDF analysis, which is commercially available by the manufacturer (Chung *et al.*, 1999).

Glaucoma patients have been shown to have significantly reduced pulsatile ocular blood flow as compared to healthy subjects (Langham *et al.*, 1991; Fontana *et al.*, 1998), and healthy ocular hypertensive subjects (Trew and Smith, 1991). Treatment of glaucoma patients with timolol has been shown either to not affect (Trew and Smith, 1991) or to lower pulsatile ocular blood flow (Langham and Romeiko, 1992). This latter result is supported by a study of the drug's effects in normal subjects also showing reduced pulsatile flow (Yoshida *et al.*, 1991). Another study has shown no change with timolol treatment in healthy eyes (Yamazaki *et al.*, 1992). Carteolol has increased pulsatile ocular blood flow in healthy eyes (Yamazaki *et al.*, 1992), while levobunolol has increased pulsatile flow in both healthy and glaucomatous eyes (Bosem *et al.*, 1992). Topical carbonic anhydrase inhibition increases ocular pulse amplitude in high tension primary open angle glaucoma (Schmidt *et al.*, 1998). Despite these studies, the relevance of pulsatile blood flow measurements in glaucoma has been questioned since the measure is believed to represent primarily choroidal circulation. Choroidal blood flow represents about 90% of the eye's circulation, of which the optic nerve head's perfusion is likely to be only a tiny percentage (Hitchings, 1991).

A number of researchers have taken advantage of color Doppler imaging to assess orbital hemodynamics in glaucoma. Galassi *et al.* used the technique in 1992 to find lower peak systolic velocities in the ophthalmic arteries of glaucomatous eyes (Galassi *et al.*, 1992). POAG patients studied

by Sergott *et al.* presented with lower peak systolic and end diastolic velocities in their ophthalmic and posterior ciliary arteries (Sergott *et al.*, 1994). Königsreuther and Michelson have also documented reduced velocities on the central retinal arteries of high tension glaucoma patients (Königsreuther and Michelson, 1994). Compared with normals, patients with NTG had lower PSV in their ophthalmic and central retinal arteries (Durcan *et al.*, 1993). Harris *et al.* found that NTG patients had significantly lower EDV and higher resistance indices in the ophthalmic arteries compared with the healthy controls at the baseline resting condition (Harris *et al.*, 1994). While breathing carbon dioxide, a potent vasodilator, healthy controls remained unchanged, whereas in patients EDV increased and resistance indices decreased such that the differences between groups were abolished. These results suggest that NTG patients may present with reversible ocular vasospasm (Harris *et al.*, 1994).

Trabeculectomy surgery was reported to improve blood flow velocities and to lower resistance in the central retinal artery and posterior ciliary arteries of glaucoma patients (Trible *et al.*, 1994).

4. OCULAR HEMODYNAMICS IN AGE-RELATED MACULAR DEGENERATION

4.1. Prevalence and Pathogenesis of Age-Related Macular Degeneration

Age related macular degeneration (AMD) is the leading cause of irreversible visual loss in the United States, occurring in over 10% of the population aged 65 to 74 years and over 25% of the population over the age of 74 years (Leibowitz *et al.*, 1980). Nonexudative AMD occurs in approximately 27% of patients over 75 years, and exudative AMD occurs in nearly 5% of this group (Klein *et al.*, 1992). Overall, approximately 10–20% of patients with nonexudative AMD progress to the exudative form, which is responsible for most of the estimated 1.2 million cases of severe visual loss from AMD (Hyman *et al.*, 1992; Tielsch *et al.*, 1995).

Several theories of pathogenesis have been proposed and these include primary RPE senescence (Eagle, 1984; Young, 1987), genetic defects such as ABCR gene mutations (which encodes a retinal rod photoreceptor) (Allikmets *et al.*, 1997) and primary ocular perfusion abnormalities (Friedman *et al.*, 1995). Traditionally, investigators have felt that senescence of the RPE, which metabolically supports and maintains the photoreceptors, leads to AMD (Eagle, 1984; Young, 1987). It has been felt that the senescent RPE accumulates metabolic debris as remnants of incomplete degradation from phagocytosed rod and cone membranes and that progressive engorgement of these RPE cells leads to drusen formation with subsequent progressive further dysfunction of the remaining RPE (Eagle, 1984; Young, 1987).

Although the theory of RPE senescence is appealing, it does not fully account for the wide variety of clinical presentations in AMD, including various forms of drusen, hyperpigmentation and RPE atrophy in nonexudative AMD as well as CNVM formation in exudative AMD. Another pathogenic theory, consequently, involves primary vascular changes in the choroid which then secondarily affect the RPE and lead to AMD; specifically, it is theorized that lipid deposition in sclera and Bruch's membrane leads to impaired choroidal perfusion, which would in turn adversely affect metabolic transport function of the retinal pigment epithelium (Friedman *et al.*, 1995; Friedman, 1997). Yet another theory involves genetic defects; for example, some investigators recently reported that 16% AMD patients in their study had a genetic defect in a gene encoding a retinal rod photoreceptor, the ABCR gene, which has also been found to be defective in Stargardt's disease; the fact that the majority of these patients did not have this mutation underscores the heterogeneous nature of this disease (Allikmets *et al.*, 1997). Other genetic factors include ancestry; persons of Caucasian ancestry are far more likely to suffer vision loss from AMD than those of African ancestry (Sommer *et al.*, 1991) or Hispanic lineage (Cruickshanks *et al.*, 1993). Investigators are also studying other hereditary dystrophies with some features similar to AMD, such as Sorsby's dystro-

phy (Peters and Greenberg, 1995), Doyne's Honeycomb retinal dystrophy (Gregory *et al.*, 1996), and autosomal dominant drusen (Heon *et al.*, 1996).

Consequently, each of these theories may play a role as AMD, with its widely varying clinical presentations, may actually represent several distinct disorders that have yet to be more clearly differentiated on a pathogenic basis; it is possible that RPE senescence represents the primary derangement in some subforms, choroidal perfusion defects represent the primary derangement in other subforms, and perhaps photoreceptor defects represent the primary defect in yet other subforms. Epidemiological risk factors including cigarette smoking (Christen *et al.*, 1996; Seddon *et al.*, 1996), blue light or sunlight exposure (Cruickshanks *et al.*, 1993) and nutritional factors (Seddon *et al.*, 1994; Mares Perlman *et al.*, 1995a) could represent environmental influences that exert a detrimental secondary effect on individuals with any of the underlying primary derangements noted above. Other hereditary/biological features that appear to predispose to AMD include light iris color and serum lipids (Mares Perlman *et al.*, 1995b).

With regard to the role of choroidal perfusion defects, it is well known that the choriocapillaris supplies the metabolic needs of the retinal pigment epithelium and the outer retina; a primary perfusion defect in the choriocapillaris could account for some of the physiologic and pathologic changes in AMD. For example, both acute ischemia and the subsequent reperfusion of the brain are associated with CNS cell death (Quigley *et al.*, 1995; Gillardon *et al.*, 1996; Leib *et al.*, 1996; Macaya, 1996; Nickell, 1996; Chen *et al.*, 1997). Cell death after ischemia occurs primarily by apoptosis, especially when the insult is mild (Gillardon *et al.*, 1996; Leib *et al.*, 1996; Macaya, 1996; Chen *et al.*, 1997). Mild ischemia is postulated to provoke precisely such a cellular event in retinal ganglion cells in glaucoma (Quigley *et al.*, 1995; Gillardon *et al.*, 1996; Leib *et al.*, 1996; Macaya, 1996; Nickell, 1996; Chen *et al.*, 1997), which is characterized by slow loss of these cells over years, and some forms of AMD (such as geographic atrophy of the RPE characterized by progressive loss of RPE cells) could have a similar pathogenesis to glaucoma.

4.2. Ocular Perfusion Defects in AMD

Some authors have suggested that delayed choroidal filling may correlate with diffuse thickening of Bruch's membrane (Pauleikhoff *et al.*, 1990). Eyes with delayed choroidal filling angiographically have been shown to harbor discrete areas of increased threshold on static perimetry (Chen *et al.*, 1992). Delayed choroidal filling has been noted angiographically in patients with exudative AMD (Boker *et al.*, 1993; Remulla *et al.*, 1995; Zhao *et al.*, 1995) and there is some evidence that choroidal blood flow is abnormal in patients with nonexudative AMD (Zhao *et al.*, 1995). One group, for example, used a technique called laser doppler flowmetry in subjects with nonexudative AMD to show that choroidal blood flow was decreased at the center of the fovea compared to a control group (Grunwald *et al.*, 1998). In addition, delayed choroidal filling appears to be independently associated with loss of vision; in one study, 38% of 32 eyes with this sign lost two or more lines of vision by two years compared to 14% of 64 eyes without this sign (Piguet *et al.*, 1992). This difference was related to the greater incidence of geographic atrophy in the patients with delayed choroidal filling; significantly, the incidence of CNVM was similar in each group of patients (Piguet *et al.*, 1992).

It is very difficult to quantify choroidal blood flow angiographically given the overlying retinal circulation and multilayered choroidal circulation that complicates analysis. One group recently used a new analysis technique based on indocyanine green angiography to compare the choroidal circulation in patients with AMD to a control group, and noted a statistically significant increased frequency of presumed macular watershed filling (PMWF), which they described as "characteristic vertical, angled, or stellate-shaped zones of early-phase indocyanine green videoangiographic hypofluorescence, assumed to be hypoperfusion, which disappeared in the early phase of the angiogram" (Ross *et al.*, 1998). They noted that 55.4% of 74 patients with AMD ver-

sus 15.0% of 20 normal control patients exhibited PMWF. They also note that 59.0% of the 61 patients with AMD-associated choroidal neovascularization exhibited PMWF and that the CNVM arose from the PMWF zone in 91.7% of these cases. This analysis approach provides valuable insight into abnormalities of choroidal circulation in AMD, although this method requires subjective assessment for the presence and location of PMWF.

Another more objective approach was employed in one pilot study performed at Indiana University. Choroidal circulation of 12 healthy eyes and 16 nonexudative AMD eyes were compared using a new, area dilution analysis technique, which has been described earlier applied to ICG angiography (Ciulla *et al.*, 1998). Six 63×63 pixel sized frames were located in the macular and peripapillary areas for choroidal blood flow measurement. After correction for eye movements, the digital image analysis system records mean intensity levels at each area over time. Fluorescence density in each block were averaged over time, graphed and analyzed for dye appearance time, maximal fluorescence and the rate of fluorescence build-up. Intensity curves (dye dilution curves) were plotted and the appearance of the ICG dye was characterized by a rise in the dilution curve. Intensity curves were analyzed by quantifying the slope of the filling portion of the curves, the amount of time required to rise 10% and 63% above baseline. The mean of 10% filling time (23.3 vs 17.8 s, $P = 0.004$) and the range of 63% filling time (2.40 vs 1.27 s, $P = 0.029$) was greater in AMD patients than in normal subjects. These results objectively imply heterogeneity of filling and decreased flow within the choriocapillaris of nonexudative AMD patients when compared to normals.

Friedman *et al.* has performed color Doppler imaging to evaluate the retrobulbar vasculature in AMD, and this group found statistically significant lower flow velocities and resistive indices of the central retinal and posterior ciliary arteries in patients with AMD compared to controls (Friedman *et al.*, 1995). This study included a heterogeneous population of both exudative and nonexudative AMD patients. In a recent study performed at Indiana University using color Doppler imaging, subjects with nonexudative AMD showed significant vascular defects in the nasal and temporal posterior ciliary arteries, which supply the choroid (Martin *et al.*, 1998). Specifically, peak systolic velocities (PSV) and end diastolic velocities (EDV) were significantly reduced in the nasal posterior ciliary artery ($P < 0.05$) and significantly reduced EDV in the temporal posterior ciliary artery ($P < 0.05$). This study demonstrates the presence of retrobulbar blood flow abnormalities in nonexudative AMD.

In summary, there appears to be a specific derangement in the choroidal circulation in patients with AMD. Vascular defects have been identified in both nonexudative and exudative AMD patients using fluorescein angiographic methods, laser doppler flowmetry, indocyanine green angiography and color Doppler imaging. Although these studies lend some support to the vascular pathogenesis of AMD, it is not possible to determine if the choroidal perfusion abnormalities play a causative role in nonexudative AMD, if they are simply an association with another primary alteration, such as a primary RPE defect or a genetic defect at the photoreceptor level, or if they are more strongly associated with one particular form of this heterogeneous disease. Further study is warranted.

5. FUTURE TREND

While the methods presented here for assessing ocular hemodynamics in glaucoma and AMD are not a complete collection, they are those likely to be encountered in the literature. A fundamental problem in comprehending the ocular blood flow literature is the difficulty in comparing the results of similar studies employing different assessment techniques. As is evident from the discussion above, each technique evaluates a portion of the ocular circulation in a unique way. Many techniques are directed at entirely different parts of the ocular vasculature.

Nevertheless, it seems that hemodynamic studies in glaucoma and AMD will only grow in

their importance. There is increasing epidemiologic and clinical evidence that suggests that intraocular pressure is not the sole pathogenic factor in glaucoma and RPE senescence is not the sole pathogenic factor in AMD. In our search for other possible contributors to the disease, circumstantial evidence of vascular involvement in glaucoma and AMD has now been joined by experimental evidence. As already mentioned, alleviating ischemia might play a central role in slowing retinal ganglion cell death by apoptosis in glaucoma and RPE dysfunction in AMD. Ocular vasospasm, impaired vascular autoregulation, decreased systemic arterial blood pressure, and reduced retinal, choroidal and retrobulbar circulation have all been reported in glaucoma. Hypertension, tobacco use and high fat diets represent risk factors in AMD, and it is intriguing that these risk factors are similar to those found in cardiovascular disease. Currently available pharmaceuticals, including topical beta blockers, topical carbonic anhydrase inhibitors, and systemic calcium channel blockers, may someday be used to minimize the macular perfusion defects in this disorder, and could theoretically maximize macular fuction. In accordance with the vascular theory of pathogenesis of age-related macular degeneration, agents such as these could possibly decrease the rate of disease progression in the early stages of this disorder.

By constantly thriving to improve and develop cutting edge technologies for evaluating ocular blood flow, their clinical availability is imminent and the ultimate beneficiary will be the patients.

REFERENCES

Allikmets, R. and Shroyer, N. *et al.* (1997) Mutation of the Stargardt disease gene (ABCR) in age-related macular degeneration. *Science* **277,** 1805–1807.

Archer, D., Krill, A.F. and Newell, F.W. (1970) Fluorescein studies of normal choroidal circulation. *Am. J. Ophthalmol.* **69,** 543.

Baker, K.J. (1966) Binding of sulfobromophthalein (BSP) sodium and indocyanine green (ICG) by plasma a(alpha)1-lipoproteins. *Proc. Soc. Exp. Biol. Med.* **122,** 957.

Behrendt, T. and Wilson, L.A. (1965) Spectral reflectance photography of the retina. *Am. J. Ophthalmol.* **59,** 1079.

Bennet, A.G., Rudnicka, A.R. and Edgar, D.F. (1994) Improvements on Littmann's method of determining the size of retinal features by fundus photography. *Graefe's Arch. Clin. Exp. Ophthalmol.* **232,** 361–367.

Boker, T. and Fang, T. *et al.* (1993) Refractive error and choroidal perfusion characteristics in patients with choroidal neovascularization and age-related macular degeneration. *Ger. J. Ophthalmol.* **2**(1), 10–13.

Bosem, M.E., Lusky, M. and Weinreb, R.N. (1992) Short-term effects of levobunolol on ocular pulsatile flow. *Am. J. Ophthalmol.* **114,** 280–286.

Bracher, D., Dozzi, M. and Lotmar, W. (1979) Measurement of vessel width on fundus photographs. *Graefe's Arch. Clin. Exp. Ophthalmol.* **211,** 35–48.

Bulpitt, C.J., Dollery, C.T. and Kohner, E.M. (1970) The marginal plasma zone in the retinal microcirculation. *Cardiovasc. Res.* **4,** 207.

Butt, Z. and O'Brien, C. (1995) Reproducibility of pulsatile ocular blood flow measurements. *J. Glaucoam.* **4,** 214–218.

Chang, E.J., Fanous, M.M. and Jocson, V.L. (1994) Reproducibility of ophthalmic artery blood flow analysis with transcranial Doppler flow spectrum vs. linear color Doppler imaging. ARVO Abstract. *Invest. Ophthalmol. Vis. Sci.* **35**(Suppl.), 1658.

Chauhan, B. C. (1995) The relationship between intraocular pressure and visual field progression in glaucoma. In *Update to Glaucoma, Blood flow and drug treatment* (ed. S. M. Drance) pp. 1–6. Kugler, Amsterdam.

Chen, J. and Fitzke, F. *et al.* (1992) Functional loss in age-related Bruch's membrane change with choroidal perfusion defect. *Invest. Ophthalmol. Vis. Sci.* **33**(2), 334–340.

Chen, J. and Graham, S. *et al.* (1997) Apoptosis repressor genes Bcl-2 and Bcl-x-long are expressed in the rat brain following global ischemia. *J. Cereb. Blood Flow Metab.* **98,** 2–10.

Cherrick, G.R., Stein, S.W. and Leevy, C.M. *et al.* (1960) Indocyanine green: observations on its physical properties, plasma decay, and hepatic extraction. *J. Clin. Invest.* **39,** 592.

Christen, W. and Glynn, R. *et al.* (1996) A prospective study of cigarette smoking and risk in age-related macular degeneration in men. *JAMA* **276,** 1147–1151.

Chung, H. S., Harris, A., Kagemann, L. and Martin, B. (1999) Peripapillary retinal blood flow in normal-tension glaucoma. *Br. J. Ophthalmol.* (in press).

Chung, H.S., Harris, A., Kagemann, L. and Evans, D.W. (1998) Choroidal hemodynamics in normal tension glaucoma as assessed by new analysis system. Second International Glaucoma Symposium, Jerusalem, Israel, pp. 41. *March* **17,** 1998.

Ciulla, T., Harris, A., Chung, H. S. and Kagemann, L. (1998) A new method for evaluating choroidal blood flow in age-related macular degeneration: area dilution analysis. *Investig. Ophthalmol. Vis. Sci.* (Suppl) in press.

Cranstoun, S.D., Petrig, B.L., Riva, C.E. and Baine, J. (1994) Optic nerve head blood flow in the human eye by laser Doppler flowmetry (LDF). ARVO Abstracts. *Invest. Ophthalmol. Vis. Sci.* **35,** 1658.

Cruickshanks, K. and Klein, R. *et al.* (1993) Sunlight and age related macular degeneration. The Beaver Dam Eye Study. *Archives of Ophthalmology* **111**(4), 514–518.

Delori, F.C., Fitch, K.A., Feke, G.T., Deupree, D.M. and Weiter, J.J. (1988) Evaluation of micrometric and microdensitometric methods for measuring the width of retinal vessel image on fundus photographs. *Graefe's Arch. Clin. Exp. Ophthalmol.* **226,** 393–399.

Duijm, H.F.A., Thomas, J., van den Berg, T.P. and Greve, E.L. (1997) A comparison of retinal and choroidal hemodynamics in patients with primary open-angle glaucoma and normal-pressure glaucoma. *Am. J. Ophthalmol.* **123,** 644–656.

Durcan, F.J., Flahary, P.M., Digre, K.B. and Lundergan, M.K. (1993) Use of color Doppler imaging to assess ocular blood flow in low tension glaucoma. ARVO Abstract. *Invest. Ophthalmol. Vis. Sci.* **34**(Suppl.), 1388.

Eagle, R.J. (1984) Mechanisms of maculopathy. *Ophthalmology* **91**(6), 613–625.

Eisenlohr, J.E., Langham, M.E. and Maumenee, A.E. (1962) Manametric studies of the pressure-volume relationship in living and enucleated eyes of individual human subjects. *Br. J. Ophthalmol.* **46,** 536–548.

Eisenlohr, J.E. and Langham, M.E. (1962) The relationship between pressure and volume changes in living and dead rabbit eyes. *Invest. Ophthalmol.* **1,** 63–77.

Flaharty, P.M., Priest, D.L. and Eaton, A.M. *et al.* (1994) Reproducibility of orbital hemodynamic parameters as measured by color Doppler imaging in normal volunteers. ARVO Abstract. *Invest. Ophthalmol. Vis. Sci.* **35**(Suppl.), 1630.

Flower, R.W. and Hochheimer, B.F. (1972) Clinical infrared absorption angiography of the choroid. *Am. J. Ophthalmol.* **73,** 458.

Flower, R.W. (1972) Infrared absorption angiography of the choroid and some observations on the effects of high intraocular pressures. *Am. J. Ophthalmol.* **74,** 600.

Fontana, L., Poinoosawmy, D., Bunce, C.V., O'Brien, C. and Hitching, R.A. (1998) Pulsatile ocular blood flow investigation in asymmetric normal tension glaucoma and normal subjects. *Br. J. Ophthalmol.* **82,** 731–736.

Friedman, E. (1997) A hemodynamic model of the pathogenesis of age-related macular degeneration. *Am. J. Ophthalmol.* **124,** 677–682.

Friedman, E. and Krupsky, S. *et al.* (1995) Ocular blood flow velocity in age-related macular degeneration. *Ophthalmology* **102**(4), 640–646.

Gabel, V.P., Birngruber, R. and Nasemann, J. (1988) Fluorescein angiography with the scanning laser ophthalmoscope. *Lasers and light in Ophthalmology* **2,** 35–40.

Galassi, F., Nuzzaci, G. and Sodi, A. *et al.* (1992) Color Doppler imaging in evaluation of optic nerve blood supply in normal and glaucomatous subjects. *Int. Ophthalmol.* **16,** 273–276.

Geeraets, W.J., Williams, R.C. and Chang, G. *et al.* (1960) The loss of light energy in retina and choroid. *Arch. Ophthalmol.* **64,** 606.

Gillardon, F. and Lenz, C. *et al.* (1996) Altered expression of Bcl-2, Bcl-x, Bax, and c-Fos colonizes with DNA fragmentation and ischemic cell damage following middle cerebral artery occlusion in rats. *Brain Res. Mol. Brain Res.* **40,** 254–260.

Gregory, C.Y. and Evans, K. *et al.* (1996) The gene responsible for autosomal dominant Doyne's honeycomb retinal dystrophy (DHRD) maps to chromosome 2p16 [published erratum appears in *Hum. Mol. Genet.* 1996 Sep; 5(9): 1390]. *Hum. Mol. Genet.* **5**(7), 1055–1059.

Grunwald, J.E. (1991) Effect of two weeks of timolol maleate treatment on the normal retinal circulation. *Invest. Ophthalmol. Vis. Sci.* **32,** 39–45.

Grunwald, J. and Hariprasad, S. *et al.* (1998) Foveolar choroidal blood flow in age-related macular degeneration. *Invest. Ophthalmol. Vis. Sci.* **39,** 385–390.

Gutoff, R.F., Berger, R.W. and Winkler, P. *et al.* (1991) Doppler ultrasonography of the ophthalmic and central retinal vessels. *Arch. Ophthalmol.* **109,** 532–536.

Harris, A., Anderson, D.R. and Pillunat, L. *et al.* (1996a) Laser Doppler flowmetry measurement of changes in human optic nerve head blood flow in response to blood gas perturbations. *J. Glaucoma* **5,** 258–265.

Harris, A., Joos, K., Kay, M., Evans, D., Shetty, R. and Martin, B. (1996b) Acute IOP elevation with scleral suction: effects on retrobulbar haemodynamics. *Br. J. Ophthalmol.* **80,** 1–5.

Harris A., Arend O. and Kagemann L. *et al.*, (1999) Dorzolamide, Visual Function and Ocular Hemodynamics in Normal-Tension Glaucoma. *J. Ocular Pharmacology and Therapeutics*. (in press).

Harris, A., Sergott, R.C. and Spaeth, G.L. *et al.* (1994) Color Doppler analysis of ocular vessel blood velocity in normal tension glaucoma. *Am. J. Ophthalmol.* **118,** 642–649.

Heon, E. and Piguet, B. *et al.* (1996) Linkage of autosomal dominant radial drusen (malattia leventinese) to chromosome 2p16–21. *Arch. Ophthalmol.* **114**(2), 193–198.

Hickam, J.B. and Frayser, R. (1997) A photographic method for measuring the mean retinal circulation time using fluorescein. *Invest. Ophthalmol.* **4,** 876–884.

Hickam, J.B. and Sieker, H.O. (1960) Retinal vascular reactivity in patients with diabetes mellitus and with arteriosclerosis. *Circulation* **22,** 243–246.

Hitchings, R. (1991) The ocular pulse. *Br. J. Ophthalmol.* **75,** 65.

Hodge, J.V., Parr, J.C. and Spears, G.F.S. (1969) Comparison of method of measuring vessel widths on retinal photographs and the effect of fluorescein injection on apparent retinal vessel caliber. *Am. J. Ophthalmol.* **68,** 1060–1068.

Hyman, L. and He, O. *et al.* (1992) Risk factors for age-related maculopathy. *Inv. Ophthalmol. Vis. Sci.* **33**(8), 548.

Jonas, J.B., Nguyen, X.N. and Naumann, G.O.H. (1989) Parapapillary retinal vessel diameter in normal and glaucoma eyes. I. Morphometric data. *Invest. Ophthalmol. Vis. Sci.* **30,** 1599–1603.

Joos, K.M., Pillunat, L.E. and Knighton, R.W. *et al.* (1994) Reproducibility of laser Doppler flowmetry (LDF)

measurements of the human optic nerve. ARVO Abstracts. *Invest. Ophthalmol. Vis. Sci.* **35,** 1659.

Kagemann, L., Harris, A., Chung, H.S., Evans, D.W., Buck, S. and Martin, B. (1998) Heidelberg retinal flowmetry: factors affecting blood flow measurement. *British J. Ophthalmol.* **82,** 131–136.

Klein, R. and Klein, B. *et al.* (1992) Prevalence of age-related maculopathy. The Beaver Dam Eye Study. *Ophthalmology* **99**(6), 933–943.

Königsreuther, K.A. and Michelson, G. (1994) Retinal hemodynamics in glaucoma. ARVO Abstract. *Invest. Ophthalmol. Vis. Sci.* **35**(suppl), 1842.

Langham, M.E. and Eisenlohr, J.E. (1963) A manometric study of the rate of fall of the intraocular pressure in living and dead eyes of human subjects. *Invest. Ophthalmol.* **2,** 72–82.

Langham, M. E., Farrel, R., Krakau, T. and Silver, D. (1991) Ocular pulsatile blood flow, hypotensive drugs, and differential light sensitivity in glaucoma. In *Glaucoma Update IV* (ed. G. K. Krieglstein) pp. 162–172. Berlin, Springer-Verlag.

Langham, M. E., Farrell, R. A. and O'Brien, V. *et al.* (1989a). Non-invasive measurement of pulsatile blood flow in the human eye. In *Ocular Blood Flow in Glaucoma* (eds. G. N. Lambrou and E. L. Greve) pp. 93–99. Berkeley, Kugler and Ghedini.

Langham, M.E., Farrell, R.A. and O'Brien, A. *et al.* (1989b) Blood flow in the human eye. *Acta Ophthalmologica* **191**(Suppl.), 9–13.

Langham, M.E. and Romeiko, W.J. (1992) The unfavorable action of timolol on ocular blood flow and vision in glaucomatous eyes. ARVO Abstract. *Invest Ophthalmol Vis Sci* **32,** 1046.

Langham, M.E. and Tomey, K.F. (1978) A clinical procedure for the measurement of ocular pulse-pressure relationship and the ophthalmic arterial pressure. *Exp. Eye Res.* **27,** 17–25.

Langham, M. E. (1987) Ocular blood flow and visual loss in glaucomatous eyes. In *Glaucoma Update III* (ed. G. K. Krieglstein) pp. 58–66. Berlin, Springer-Verlag.

Leib, S. and Kim, Y. *et al.* (1996) Reactive oxygen intermediates contribute to necrotic and apoptotic neuronal injury in an infant rat model of bacterial meningitis due to group B streptococci. *J. Clin. Invest.* **98,** 2632–2639.

Leibowitz, H. and Krueger, D. *et al.* (1980) The Framingham Eye Study monograph: an ophthalmological and epidemiological study of cataract, glaucoma, diabetic retinopathy, macular degeneration, and visual acuity in a general population of 2631 adults, 1973–1975. *Surv. Ophthalmol.* **24**(Suppl.), 335–610.

Lieb, W.E., Cohen, S.M. and Merton, D.A. *et al.* (1991) Color Doppler imaging of the eye and orbit: technique and normal vascular anatomy. *Arch. Ophthalmol.* **109,** 527–531.

Macaya, A. (1996) Apoptosis in the nervous system. *Rev. Neurol.* **24,** 1356–1360.

Mares Perlman, J. and Brady, W. *et al.* (1995a) Dietary fat and age related maculopathy [see comments]. *Archives of Ophthalmology* **113**(6), 743–748.

Mares Perlman, J. and Brady, W. *et al.* (1995b) Serum antioxidants and age related macular degeneration in a population based case control study. *Archives of Ophthalmology* **113**(12), 1518–1523.

Martin, B., Harris, A., Chung, H. S. and Kagemann, L. (1998) Reduced posterior ciliary artery flow velocities in age-related macular degeneration. *Investig. Ophthalmol. Vis. Sci.* (Suppl) in press.

Maumenee, A.E. (1968) Fluorescein angiography in the diagnosis and treatment of lesions of the ocular fundus (The 1968 Doyne Lecture). *Trans. Ophthalmol. Soc. UK* **88,** 529.

Michelson, G., Schmauss, B. and Langhans, M.J. *et al.* (1996) Principle, validity, and reliability of scanning laser doppler flowmetry. *J. Glaucoma* **5,** 99–105.

Michelson, G. and Schmauß, B. (1995) Two-dimensional mapping of the perfusion of the retina and optic nerve head. *Br. J. Ophthalmol.* **79**(12), 1126–1132.

Nagel, E., Vilser, W., Lindloh, C. and Klein, S. (1992) Messung retinaler Gefaßdurchmesser mittels Scanning-Laser Ophthalmoskop und Computer. *Ophthalmologe* **89,** 432–436.

Nakahashi, K. (1990) Macular blood flow measured by blue field entoptic phenomenon. *Jpn. J. Ophthalmol.* **24,** 331–337.

Nasemann, J. E. and Müller, M. (1990) Scanning laser angiography. In *Scanning Laser Ophthalmoscopy and Tomography* (eds. J. E. Nasemann and R. O. W. Burk) pp. 63–80. München, Quintessenz.

Nickell, R.W. (1996) Retinal ganglion cell death in glaucoma: the how, the why, and the maybe. *J. Glaucoma* **5,** 345–356.

Pauleikhoff, D. and Chen, J. *et al.* (1990) Choroidal perfusion abnormality with age-related Bruch's membrane change. *Am. J. Ophthalmol.* **109**(2), 211–217.

Peters, A. and Greenberg, J. (1995) Sorsby's fundus dystrophy. A South African family with a point mutation on the tissue inhibitor of metalloproteinases-3 gene on chromosome 22. *Retina* **15**(6), 480–485.

Petrig, B.L. and Riva, C.E. (1988) Retinal laser Doppler velocimetry: towards its computer-assisted use. *Appl. Optics* **27,** 1126–1134.

Piguet, B. and Palmvang, I. *et al.* (1992) Evolution of age-related macular degeneration with choroidal perfusion abnormality. *Am. J. Ophthalmol.* **113**(6), 657–663.

Plesch, A., Klingbeil, U., Rappl, W., Schrödel, C. (1990) Scanning ophthalmic imaging. In *Scanning Laser Ophthalmoscopy and Tomography* (eds. J. E. Nasemann and R. O. W. Burk) pp. 23–33. München, Quintessenz.

Pourcelot, L. (1975) Indications de l'ultrasonographie Doppler dans l'etude des vaisseaux peripheriques. *Revue du Praticien* **25,** 4671–4680.

Powis, R.L. (1988) Color flow imaging: understanding its science and technology. *J. Diag. Med. Ultrasound* **4,** 236–245.

Quigley, H.A., Nickell, R.W. and Kerrigan, L.A. *et al.* (1995) Retinal ganglion cell death in experimental glaucoma and after axotomy occurs by apoptosis. *Invest. Ophthalmol. Vis. Sci.* **36,** 774–786.

Quigley, H.A. and Vitale, S. (1997) Models of open-angle glaucoma prevalence and incidence in the United States. *Invest. Ophthalmol. Vis. Sci.* **38,** 83–91.

Ramalho, P.S. and Dollery, C.T. (1968) Hypertensive retinopathy: caliber changes in retinal blood vessels following

blood pressure reduction an inhalation of oxygen. *Circulation* **37,** 580–588.

Rehkopf, P., Friberg, T. R., Mandarino, L., Warnicki, J., Finegold, D., Capozzi, D. and Horner, J. (1990) Retinal circulation time using scanning laser ophthalmoscope-image processing techniques. In *Scanning Laser Ophthalmoscopy and Tomography* (eds. J. E. Nasemann and R. O. W. Burk) pp. 81–89. München, Quintessenz.

Remulla, J. and Gaudio, A. *et al.* (1995) Foveal electroretinograms and choroidal perfusion characteristics in fellow eyes of patients with unilateral neovascular age-related macular degeneration. *Br. J. Ophthalmol.* **79**(6), 558–561.

Riva, C.E., Harino, S., Petrig, B.L. and Shonat, R.D. (1992) Laser Doppler flowmetry in the optic nerve. *Exp. Eye Res.* **55,** 499–506.

Riva, C. E., Petrig, B. O. and Grunwald, J. E. (1989a). Retinal blood flow. In *Laser-Doppler Flowmetry* (eds. A. P. Shepherd and P. Å. Öberg) pp. 349–383. Boston, Kluwer Academic Publishers.

Riva, C. E., Shonat, R. D., Petrig, B. L., Pournaras, C. J. and Barnes, J. B. (1989b) Noninvasive measurement of the optic nerve head circulation. In *Ocular Blood Flow in Glaucoma: Means, Methods, and Measurements* (eds. G. N. Lambrou and E. L. Greve) pp. 129–134. Berkley, Kugler and Ghedini.

Riva, C.E., Pournaras, C.J., Poitry-Yamate, C.L. and Petrig, B.L. (1990) Rhythmic changes in velocity, volume, and flow of blood in the optic nerve head tissue. *Microvasc. Res.* **40,** 36–45.

Ross, R. and Barofsky, J. *et al.* (1998) Presumed macular choroidal watershed vascular filling, choroidal neovascularization, and systemic vascular disease in patients with age-related macular degeneration. *Am. J. Ophthalmol.* **125,** 71–80.

Schappert, S. M. (1995) Office visits for glaucoma: United states, 1991–1992. Public Health Service, centers for disease control and prevention. Advance Data. Hyattsville, MD: National center for health statistics; **262,** 1–13.

Schmidt, K.G., von Ruckmann, A. and Pillunat, L.E. (1998) Topical carbonic anhydrase inhibition increases ocular pulse amplitude in high tension primary open angle glaucoma. *Br. J. Ophthalmology* **82,** 758–762.

Seddon, J. and Ajani, U. *et al.* (1994) Dietary carotenoids, vitamins A, C and E, and advanced age-related macular degeneration. *JAMA* **272,** 1413–1420.

Seddon, J. and Willet, W. *et al.* (1996) A prospective study of cigarette smoking and age-related macular degeneration in women. *JAMA* **276,** 1141–1146.

Sergott, R.C., Aburn, N.S. and Trible, J.R. *et al.* (1994) Color Doppler Imaging: methodology and preliminary results in glaucoma [Published erratum appears in *Surv. Ophthalmol.* 1994 **39**(2): 165]. *Surv. Ophthalmol.* **38**(Suppl.), S65–70.

Sieker, H.O. and Hickam, J.B. (1955) Normal and impaired retinal vascular reactivity. *Circulation* **7,** 79–83.

Sieker, H.O., Hickman, J.B. and Gibson, J.F. (1955) The relationship between impaired retinal vasculature reactivity and renal function in patients with degenerative vascular disease. *Circulation* **12,** 64–68.

Silver, D.M., Farrell, R.A. and Langham, M.E. *et al.* (1989) Estimation of pulsatile ocular blood flow from intraocular pressure. *Acta Ophthalmologica* **191**(Suppl.), 25–29.

Sommer, A. and Tielsch, J. *et al.* (1991) Racial differences in the cause-specific prevalence of blindness in East Baltimore. *N. Engl. J. Med.* **325**(20), 1440–1442.

Taylor, K.J.W. and Holland, S. (1990) Doppler US part I: Basic principles, instrumentation, and pitfalls. *Radiology* **174,** 297–307.

Tielsch, J. and Javitt, J. *et al.* (1995) The prevalence of blindness and visual impairment among nursing home residents in Baltimore [see comments]. *N. Engl. J. Med.* **332**(18), 1205–1209.

Tielsh, J.M. (1996) The epidemiology and control of open-angle glaucoma: a population-based perspective. *Ann. Rev. Public Health* **17,** 121–136.

Trew, D.R. and Smith, S.E. (1991) Postural studies in pulsatile ocular blood flow: II. Chronic open angle glaucoma. *Br. J. Ophthalmol.* **75,** 71–75.

Trible, J.R., Sergott, R.C. and Spaeth, G.L. *et al.* (1994) Trabeculectomy is associated with retrobulbar hemodynamic changes. *Ophthalmology* **101,** 340–351.

Von Bibra, H., Stempfle, H.U. and Poll, A. *et al.* (1990) Genauighkeit verschiedener Dopplertechniken in der Erfassung von Flußgeschwindigkeiten Untershuchgen *in vitro*. *Z. Kardiol.* **79,** 73–82.

Von Helmholz, H. (1951) Beschreibung eines Augen-Spiegels zur Untersuchung der Netzhaut im lebenden Auge. Berlin, A. forstner, 1851 (Description of an ophthalmoscope for examining the retina of the living eye. Hollenhorst RW trans). *Arch. Ophthalmol.* **46,** 565–583.

Wald, G. (1949) The photochemistry of vision. *Doc. Ophthalmol.* **3,** 94.

Webb, R.H., Hughes, G.W. and Delori, F.C. (1987) Confocal scanning laser ophthalmoscope. *Appl. Opt.* **26,** 1492–1499.

Webb, R.H., Hughes, G.W. and Pomerantzeff, O. (1980) Flying spot TV ophthalmoscope. *Appl. Opt.* **19,** 2991–2997.

Williamson, T.H. and Harris, A. (1996) Color Doppler ultrasound imaging of the eye and orbit. *Surv. Ophthalmol.* **40,** 255–267.

Williamson, T.H. (1994) What is the use of ocular blood flow measurement? *Br. J. Ophthalmol.* **78,** 326.

Wolf, S., Arend, O. and Reim, M. (1994) Measurement of retinal hemodynamics with scanning laser ophthalmoscopy: reference values and variation. *Surv. Ophthalmol.* **38**(suppl), S95–S100.

Wolf, S., Arend, O., Sponsel, W.E. and Schulte, K. *et al.* (1993) Retinal hemodynamics using scanning laser ophthalmoscopy and hemorheology in chronic open-angle glaucoma. *Ophthalmology* **100,** 1561–1566.

Yamazaki, S., Baba, H. and Tokoro, T. (1992) Effects of timolol and carteolol on ocular pulsatile blood flow. *Acta Soc. Ophthalmol. Jpn.* **96,** 973–977.

Yang, Y.C., Hulbert, M.F.G. and Batterbury, M. *et al.* (1997) Pulsatile ocular blood flow measurements in healthy eyes: reproducibility and reference values. *J. Glaucoma* **6,** 175–179.

Yoshida, A., Feke, G.T. and Ogasawara, H. *et al.* (1991) Effect of timolol on human retinal, choroidal, and optic nerve head circulation. *Ophthalmic Res.* **23,** 162–170.

Young, R. (1987) Pathophysiology of age-related macular degeneration. *Surv. Ophthalmol.* **31**(5), 291–306.

Zhao, J. and Frambach, D. *et al.* (1995) Delayed macular choriocapillary circulation in age-related macular degeneration. *Int. Ophthalmol.* **19,** 1–12.